

# Uplift age and rates of the Gurvan Bogd system (Gobi-Altay) by apatite fission track analysis

R. Vassallo<sup>a,\*</sup>, M. Jolivet<sup>a</sup>, J.-F. Ritz<sup>a</sup>, R. Braucher<sup>b</sup>, C. Larroque<sup>c</sup>,  
C. Sue<sup>d</sup>, M. Todbileg<sup>e</sup>, D. Javkhlanbold<sup>e</sup>

<sup>a</sup> *Géosciences Montpellier, CNRS-UMII UMR 5243, Université Montpellier II, Montpellier, France*

<sup>b</sup> *CEREGE, UMR 6635, Europole Méditerranéen de l'Arbois, Aix-en-Provence, France*

<sup>c</sup> *Géosciences Azur, UMR 6526, Sophia-Antipolis, Valbonne, France*

<sup>d</sup> *Département de Géologie, Université de Neuchâtel, Switzerland*

<sup>e</sup> *Mongolian University of Science and Technology, Ulaan Baatar, Mongolia*

Received 17 March 2006; received in revised form 26 April 2007; accepted 28 April 2007

Available online 8 May 2007

Editor: C.P. Jaupart

## Abstract

The dating of the uplift onset of the Mongolian mountain ranges, the northernmost relief associated with the India-Eurasia convergence, is a fundamental issue to better understand the mechanisms of propagation of the Cenozoic transpressive deformation in Central Asia. Using apatite fission tracks we determined the timing and strain rates of the tectonics affecting the Gurvan Bogd system, in the Gobi-Altay, since the Middle Mesozoic to the Late Cenozoic. The region was firstly affected by a Lower–Middle Jurassic tectonic phase, characterized by a vertical crustal movement larger than 2 km. Then followed a protracted period without major crustal vertical movements until the last uplift phase. The peneplanation of the Jurassic relief produced an erosional surface that has undergone negligible denudation or sedimentation for more than 100 Ma. This same surface corresponds to the present summit plateaux of the massifs, standing about 2000 m above the surrounding region, which corresponds to the vertical movement produced by the ongoing uplift. Modelling of fission track data from the massifs of Ih Bogd and Baga Bogd shows that this uplift phase probably started at  $5 \pm 3$  Ma. The Gobi-Altay mountain range appears therefore as one of the youngest mountain ranges in Central Asia, which is consistent with the idea of a northward propagation of the transpressional deformation from the Himalayan front to the Siberian craton. The Cenozoic uplift rate of the massifs is estimated to be between 0.25 and 1 mm/yr, which is slightly higher than the upper Pleistocene vertical slip rates of the bordering faults. This suggests that thrust faults observed within the massifs would increase the uplift rate inside the massifs compared to the uplift rate determined at their boundaries.

© 2007 Elsevier B.V. All rights reserved.

*Keywords:* Central Asia; Mongolia; Mesozoic–Cenozoic tectonics; fission tracks; massifs uplift; summit plateau

## 1. Introduction

The Asian continent has been undergoing widespread tectonic deformation since India-Eurasia collision began

at the Paleocene–Eocene (Patriat and Achache, 1984; Besse et al., 1984; Patzelt et al., 1996). A transpressive regime from the Himalayan front up to the Siberian craton involves a lithospheric NNW-SSE shortening over a 3000-km-wide area (Tapponnier and Molnar, 1979) (Fig. 1A). Within this region, the deformation of the upper crust results in the building of linear mountain

\* Corresponding author.

E-mail address: [vassallo@gm.univ-montp2.fr](mailto:vassallo@gm.univ-montp2.fr) (R. Vassallo).

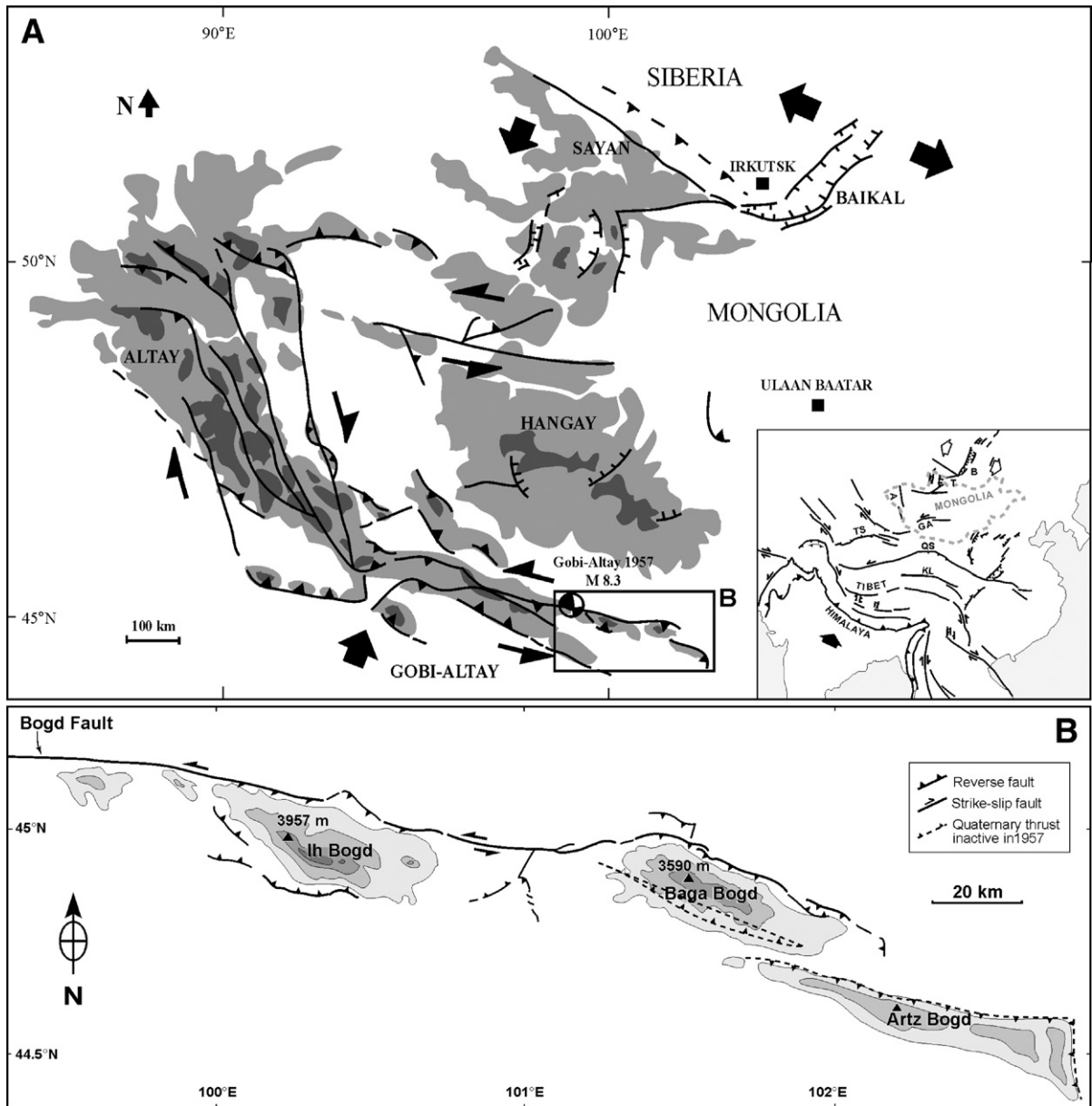


Fig. 1. (A) Simplified map of the main mountain ranges and associated active faults in Mongolia, modified after Vassallo et al. (2005). In the small frame (modified after Ritz et al. (2003)), sketch of the main Quaternary faults and mountain ranges in Central Asia. Symbols: B—Baikal, T—Tunka, A—Altay, GA—Gobi-Altay, TS—Tien Shan, QS—Qilian Shan, KL—Kun Lun. (B) Close-up of the Gurvan Bogd system in the Gobi-Altay mountain range.

ranges controlled by the activity of large strike-slip faults associated with smaller oblique or reverse faults.

The age of the onset of the transpressive deformation in Central Asia between the Kunlun range and Lake Baikal (Fig. 1A) is still poorly constrained. In the southern part of this region, several studies based on stratigraphy, sediment mass balances, thermochronology and magnetostratigraphy have allowed dating and

quantification of the uplift of these mountain ranges. The first phase of the intra-continental deformation started in north Tibet, with the onset of the uplift of the Kunlun Shan and Qilian Shan mountain ranges, in Eocene–Oligocene times (Jolivet et al., 2001; Wang et al., 2004). The mountain building process then moved northward to the Tien Shan, where the first main uplift episode probably occurred during the Middle Miocene

(Avouac et al., 1993; Métivier and Gaudemer, 1997; Sobel and Dumitru, 1997; Bullen et al., 2001; Charreau et al., 2005). This transpressive regime would have reached the northernmost part of Central Asia, the Baikal rift system, very recently. Several evidences of fault kinematics inversions in the Tunka basin suggest that this area has been undergoing transpression since Middle Pleistocene times (Larroque et al., 2001; Arjannikova et al., 2004). These data would support the idea that the crustal deformation propagates, at the geological time scale, from the Himalayan collision front to the still undeformed Siberian craton.

However, between the Tien Shan and the Tunka area, the age of uplift of the Altay and the Gobi-Altay in Western Mongolia (Fig. 1A) is still poorly known. The lack of well-dated Cenozoic deposits affected by the last deformation within these ranges does not allow a precise stratigraphic analysis. The dating of the massifs uplift is mainly based on their morphologic characteristics. Massifs are characterized by perched remnant erosional surfaces such as flat summit plateaux culminating at ~4000 m or uplifted piedmonts on the mountain flanks. Because of the preservation of such morphologic features from erosion, authors like Florensov and Solonenko (1965) and Baljinnnyam et al. (1993) proposed that these uplifted massifs should be no more than 1 or 2 Ma in age. Nevertheless, without a better quantification of the erosional processes, this age cannot be constrained and could also be much higher, up to one order of magnitude greater, like proposed by Ritz et al. (2003) from a morphotectonic study on the Ih Bogd massif (Gurvan Bogd system, Gobi-Altay, Figs. 1B and 2A). Assuming that the bordering faults absorb the totality of the shortening, Ritz et al. (2003) extrapolated the vertical slip rates found for the Holocene–upper Pleistocene to the geological time-scale and estimated that to create the present relief of ~2000 m the massif uplift should have started between 2 and 18 Ma. Recently, Vassallo et al. (2005) and Ritz et al. (2006) showed that the higher limit for the vertical fault slip rate is actually ~5 times smaller than previously thought, leading to a minimum age of 10 Ma for this massif.

To better constrain the age of the onset of uplift in the Gobi-Altay region, we used apatite fission track analysis, which allows dating the cooling events affecting the first few kilometers of the crust. The Mongolian ranges are associated with transpressional mountain building processes with massifs up to 3000 to 4000 m high located within restraining bends along large strike-slip faults (Cunningham et al., 1996; Cunningham, 2005). These massifs rise between 1500 m and

2000 m above their immediate piedmonts. The Gurvan Bogd system presents strong relief. More importantly, deep river incision allows sampling large vertical profiles in the core of the massifs. Gurvan Bogd thus represents one of the most suitable sites to look for the Cenozoic uplift event.

Moreover, the quaternary vertical slip rates along the faults bordering the massifs are well constrained by several morphotectonic studies based on  $^{10}\text{Be}$  dating of faulted alluvial fans (Ritz et al., 2003, 2006; Vassallo et al., 2005; Hanks et al., 1997; Carretier, 2000). This will allow us to compare the long-term general uplift of the massifs with the brittle deformation accommodated by the active faults on a smaller time-scale.

## 2. Tectonic and geomorphologic context

The Gurvan Bogd system, which constitutes the easternmost part of the Gobi-Altay, is a 300-km-long mountain range trending N100°E composed of three linear massifs (Figs. 1B and 2). These massifs (Ih Bogd, Baga Bogd and Artz Bogd) correspond to restraining bends associated with the left-lateral strike-slip Bogd fault and present reverse faulting on both northern and southern sides (Bayasgalan et al., 1999). A large part of this fault system broke recently during the M 8.1 1957 Gobi-Altay earthquake (Kurushin et al., 1997). The presence of well-developed flat horizontal summit surfaces (Fig. 3), besides suggesting a young morphologic age for these massifs, implies that their uplift is mainly accommodated by the brittle deformation along the bordering faults, even though a regional uplift cannot be excluded. Moreover, the bordering faults should have similar long-term vertical slip rates in order to keep these surfaces horizontal. This last assumption is confirmed by the  $^{10}\text{Be}$  morphotectonic studies on alluvial faulted fans along the massifs that yield upper Pleistocene vertical rates of ~0.1–0.2 mm/yr for all the segments studied (Vassallo et al., 2005; Ritz et al., 2006).  $^{10}\text{Be}$  data within the study area are only available for the alluvial fan surfaces of the Gurvan Bogd piedmont, for which they show low erosion rates in the order of few m/Ma (Vassallo et al., 2005).

Within these massifs, we observed faults trending N100–110°E sub-parallel to the active Bogd strike-slip fault (Fig. 2). These faults are correlated with perched ancient piedmonts and define a “staircase” morphology. Along the same faults, the main drainage basins appear left-laterally displaced. In the Bitut valley, along one of these faults, a Quaternary abandoned alluvial terrace is overthrust by the bedrock (Fig. 4). Therefore, it appears that these internal faults, which

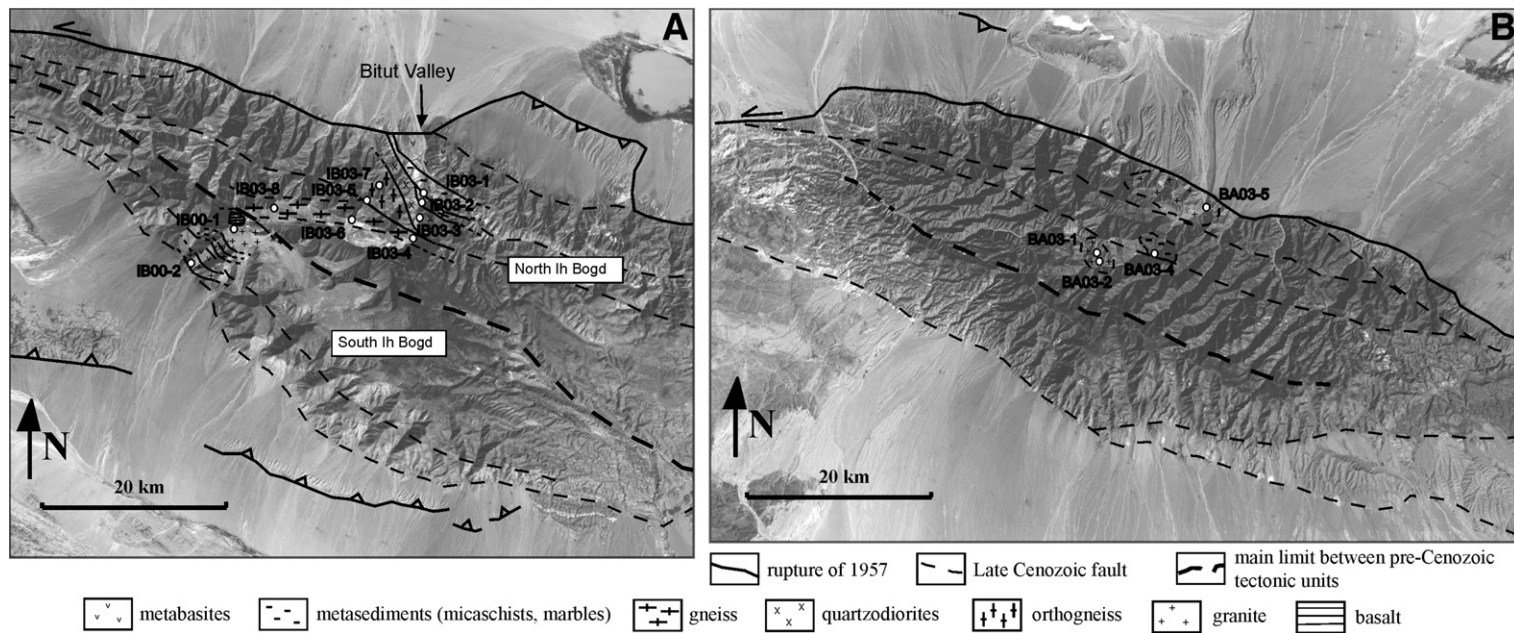


Fig. 2. Landsat images of the massifs of Ih Bogd (A) and Baga Bogd (B) with geological and structural sketch map after fieldwork and satellite images. The localities of the fission track samples are also given.



Fig. 3. Picture of the summit plateau of Ih Bogd massif. The highest point at 3957 m corresponds to a lava flow overlying the peneplanation surface in the western part of the plateau. This surface horizontally cuts the two main Pre-Cenozoic tectonic units comprising the massif.

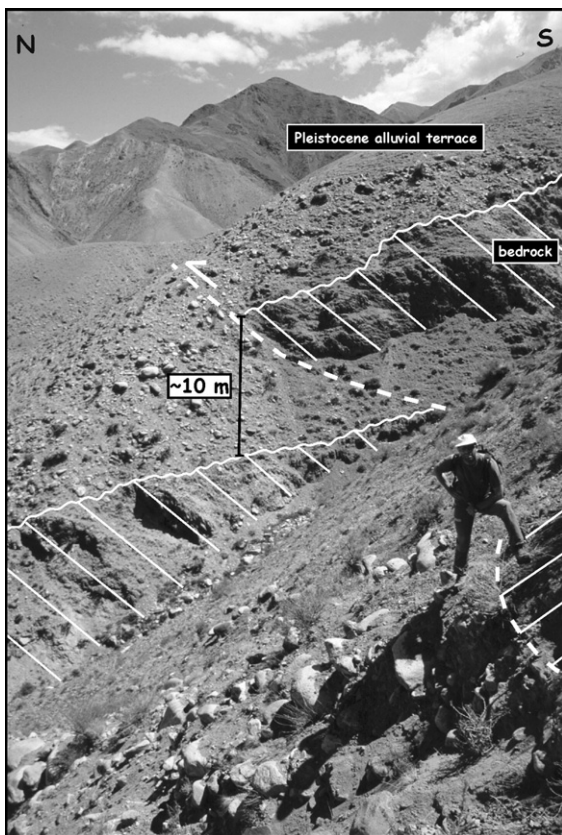


Fig. 4. Picture showing a Pleistocene alluvial terrace affected by thrusting inside the massif. The faulting corresponds to one of the main steps observed in the topography at the massif scale.

have the same geometries and kinematics as the active bordering faults, have been active during the ongoing uplift event.

### 3. Fission tracks analysis: sampling and methodology

The basement of the Gurvan Bogd massifs is composed of a large variety of lithologies (granites, gneisses, syenites, schists, diorites and metabasalts) inherited from the complex geological history that affected the region (Fig. 2). The occurrence of apatite-rich granitoids from an altitude of  $\sim 2000$  m at the heart of the massifs up to the summit plateaux (3500–4000 m) in areas of a few  $\text{km}^2$ , allowed us to sample the bedrock over sub-vertical sections of nearly 2 km at Ih Bogd and 1 km at Baga Bogd. The altitude of the samples was measured using a portable GPS and 1/100,000 Russian topographic maps, with precision in the order of 50 m. This sampling strategy allows comparing the distribution of the fission track ages with the relative altitudes of the bedrock in order to estimate the average rates and amplitudes of the cooling events (i.e. the uplift and denudation rates).

Variations in the cooling rates (i.e. in the slope of the age/altitude plot) can be interpreted in terms of erosion or tectonic events. However, the fission track ages integrate the whole thermal history of the rocks between ca. 110 and 60 °C. To better constrain the age of thermal events within the massif, reverse modelling of track lengths distribution has been performed using the AFTSolve software (Ketchum et al., 2000) and the

Ketcham et al. (1999) annealing model. These models are only valid within the fission track Partial Annealing Zone or PAZ (60 to 110 °C).

Apatites grains were mounted on a glass slide, ground, polished and etched in 6.5% HNO<sub>3</sub> for 45 s at 20 °C, in order to reveal natural fission tracks. Then, to produce induced fission tracks, apatite mounts were irradiated at the ANSTO facility, Lucas Heights, Australia, with a thermal neutron flux ( $10^{16}$  n/cm<sup>2</sup>) using a mica sheet as an external detector (Hurford and Green, 1983). Fission tracks were counted on a Zeiss Axioplan 2 microscope, using a magnification of 1250 under dry objective. The FT ages were calculated following the method recommended by Hurford (1990), using the zeta calibration method (Hurford and Green, 1983) with a zeta value of  $343 \pm 3$  (R.V.) obtained on Mt Dromedary standard (Green, 1985). Ages were calculated using the Trackkey software<sup>®</sup> (Dunkl, 2002). Ages quoted are central fission track ages with  $2\sigma$  errors. Dpar (fission track diameter) measurements were performed in order to quantify the Cl and F content of the apatite crystals (e.g. O'Sullivan and Parrish, 1995; Barbarand et al., 2003). Dpar values were then used as input parameters in the AFTSolve models.

#### 4. Results

Thirteen samples from Ih Bogd and Baga Bogd massifs were analysed. For Ih Bogd, the fission track ages range between  $195 \pm 21$  Ma and  $139 \pm 15$  Ma (Table 1 and Fig. 5A). Two different geological units, a northern metamorphic formation and a southern metabasitic-granitic complex, are cut by the same peneplanation surface and show similar ages (Figs. 2A and 3). This implies that these units have been uplifted at the present position as a unique block, and that differential vertical movements that may have occurred along the main fault zone existing between them before the ongoing uplift are not registered by the fission tracks thermochronometer. The northern unit, where we concentrated most of our analysis, shows homogeneous fission track ages of 160–170 Ma from the summit down to 2050 m. The two lowest samples (IB03-1 and IB03-2), situated at 2000 m and 1950 m have slightly younger fission track ages of  $151 \pm 9$  Ma and  $139 \pm 15$  Ma. For the southern unit we only have two data from the summit plateau (IB00-1) and from the southern flank of the massif (IB00-2). Like for the northern profile, fission track central ages decrease downward from  $195 \pm 21$  Ma to  $167 \pm 14$ . Both profiles are consistent in regard of the age-altitude data.

For this massif we also did attempt to carry out apatite U-Th/He dating on some samples along the profile. However, ages do not show a coherent vertical distribution and are in some cases illogically older than the fission track corresponding ages. We therefore invoke a perturbation of this low-temperature thermochronometer by changes in the properties of retention of the He in apatites through time over long and slow cooling histories (e.g. (Fitzgerald et al., 2006; Shuster et al., 2006; Green et al., 2006)).

As concerns the Baga Bogd massif, its internal structure, as well as that of Ih Bogd, appears to be formed by two main tectonic units. The watershed separates a northern domain characterized by well-developed valleys and relatively gentle slopes from a much narrower and steeper southern domain that presents remnants of a flat erosional summit surface (Fig. 2B). Due to difficult access, sampling was concentrated on the northern unit, along one of the main valleys of the massif. Fission track ages range from  $141 \pm 25$  Ma to  $116 \pm 13$  Ma (Table 1 and Fig. 5A). Fission track ages of this structural unit, once again, show a well-established linear correlation against the altitude, even though error margins do not allow to precisely calculate the slope of the regression curve.

Dpar vary from  $2.0 \pm 0.2$  to  $3.1 \pm 0.3$   $\mu\text{m}$  for Ih Bogd samples and from  $1.9 \pm 0.1$  to  $2.2 \pm 0.1$   $\mu\text{m}$  for Baga Bogd samples (Table 1). Fig. 5C and D show that a minor correlation between Dpar and the central fission track ages or the mean track lengths may exist, especially when all the samples from the different massifs are plotted together. However, the limited range of Dpar and the weak correlations in each individual massif suggest that compositional effects do not significantly affect the data and can be ignored. In other words, variations either in age or track lengths distribution are related to thermal events rather than chemical variations between samples. One exception is IB03-3, which has a Dpar of  $3.1 \pm 0.3$   $\mu\text{m}$  indicative of a higher Cl content (e.g. (Barbarand et al., 2003)). This can explain its higher central fission track age of  $186 \pm 20$  Ma that does not fit with the rest of the samples distribution.

The mean track length (MTL) of the samples, in both massifs and for each individual unit, increases with the altitude (Table 1 and Fig. 5B). Values range from  $11.1 \pm 0.2$  to  $13.8 \pm 0.1$   $\mu\text{m}$  between 1950 and 3650 m for the northern profile of Ih Bogd, from  $11.6 \pm 0.2$  to  $12.4 \pm 0.2$   $\mu\text{m}$  between 2740 and 2850 m for the southern profile of Ih Bogd and from  $11.3 \pm 0.2$  to  $11.8 \pm 0.2$   $\mu\text{m}$  between 2150 and 2500 m for the northern unit of Baga Bogd. MTLs are also well correlated with the fission

Table 1  
Results of the fission track analysis

Sample	Altitude (m)	Number of grains	Standard track density ( $\times 10^5 \text{ cm}^{-2}$ ) (counted)	$\rho_s$ ( $\times 10^5 \text{ cm}^{-2}$ ) (counted)	$\rho_t$ ( $\times 10^5 \text{ cm}^{-2}$ ) (counted)	[U] (ppm)	$P(\chi^2)$ (%)	Var (%)	Central age (Ma)	Uncertainty $2\sigma$ (Ma)	MTL ( $\mu\text{m}$ ) (counted)	Uncertainty $1\sigma$ ( $\mu\text{m}$ )	D-Par ( $\mu\text{m}$ )	Uncertainty $1\sigma$ ( $\mu\text{m}$ )
IB00-1	3900	20	10.9 (5327)	20.5 (180)	20.1 (177)	22.2	100	1	195	21	12.4 (60)	0.2	2.0	0.2
IB00-2	2740	20	8.9 (6331)	9.7 (294)	9.2 (278)	11.3	100	1	167	14	11.6 (100)	0.2	2.0	0.1
IB03-1	1950	20	12.1 (10887)	7.6 (141)	11.3 (210)	12.1	99	2	139	15	11.1 (100)	0.2	2.0	0.2
IB03-2	2000	20	11.8 (10887)	15.6 (487)	20.6 (647)	21.7	83	0	151	9	11.7 (99)	0.2	2.4	0.1
IB03-3	2050	20	11.4 (10887)	6.2 (174)	6.4 (181)	7.6	98	4	186	20	12.1 (67)	0.2	3.1	0.3
IB03-4	2250	20	10.7 (10887)	19.0 (728)	20.4 (783)	22.7	42	9	169	10	12.3 (100)	0.2	2.2	0.1
IB03-5	2800	20	12.0 (10364)	12.3 (678)	14.7 (813)	14.6	85	1	170	9	12.8 (100)	0.1	2.0	0.1
IB03-6	3200	20	10.4 (10887)	12.6 (709)	14.2 (800)	16.8	86	4	156	8	13.5 (100)	0.1	2.6	0.1
IB03-7	2500	20	10.0 (10887)	15.5 (901)	15.7 (913)	19.8	39	4	172	10	12.2 (100)	0.1	2.7	0.1
IB03-8	3650	20	9.8 (10887)	11.2 (303)	10.6 (287)	14.3	97	5	176	14	13.8 (100)	0.1	2.5	0.1
BA03-1	3000	20	11.8 (10364)	5.6 (53)	8.0 (75)	10.1	100	0	141	25			2.0	0.2
BA03-2	2800	23	11.4 (10364)	16.8 (166)	25.4 (251)	27.2	100	3	128	13			1.9	0.1
BA03-4	2500	20	11.0 (10364)	8.0 (199)	11.7 (293)	13.0	100	1	127	12	11.8 (100)	0.2	2.2	0.1
BA03-5	2150	20	10.7 (10364)	6.3 (136)	10.0 (214)	12.0	100	0	116	13	11.3 (88)	0.2	2.0	0.1

$\rho_s$  and  $\rho_t$  represent sample spontaneous and induced track densities;  $P(\chi^2)$  is the probability of  $\chi^2$  for  $\nu$  degrees of freedom (where  $\nu$  is the number of crystals). Zeta CNS apatite =  $343 \pm 3$  (R. V.). Samples were irradiated at the ANSTO facility, Australia. MTL of samples BA03-1 and IB03-2 could not be measured because of the lack of confined fission tracks.

track ages, except for sample IB03-3. For each of the three identified units, the remarkable coherence between the distribution of the MTLs against the altitude and central age implies that all of them were exhumed through the PAZ as a unique and untilted block, in which all the samples kept their relative vertical positions.

Cooling histories obtained from track lengths modelling all display similar patterns (Fig. 6). All the samples in both massifs are affected by a cooling event that occurred in the Lower–Middle Jurassic. Since this event was recorded on the whole vertical section of the northern unit of Ih Bogd, it must have produced a vertical crustal movement of at least 2 km. The cooling paths of the lower samples (IB03-1, IB03-2, BA03-5 and BA03-4) show that a long ( $> 100$  Ma) stable period without major variation in temperature has followed (Fig. 6C, D, F and G). Eventually, these samples recorded a cenozoic cooling event that can be correlated with the last and still ongoing uplift phase and relief building. This phase is marked by an abrupt inflexion of the cooling paths clearly contained in the PAZ, which defines the validity zone of the model—excepted for BA03-4, the highest sample among the four, for which the inflexion is smoother. Their respective cooling paths are very similar and the inflexion occurs between 8 and 2 Ma (Fig. 6C, D and G).

## 5. Discussion

The fission track analysis carried out within the Ih Bogd and Baga Bogd massifs allowed us to reconstruct the geological history of the shallow crust of the Gurvan Bogd region over a period of time ranging from the Middle Mesozoic to the Late Cenozoic. Samples from Ih Bogd northern unit (from 1950 m to 3650 m, or to 3850 m if we consider the overlying rocks of the same unit), all present the same Middle Jurassic central ages except for the two lowest samples, which are slightly younger. This means that the main upper part of this section has remained at temperatures lower than 60 °C since the Jurassic cooling episode. On the contrary, until the last uplift, the two lowest samples of the pile were situated deep enough to be rejuvenated within the PAZ. In other words, this section was situated between the surface and the upper part of the PAZ before the last uplift phase (Fig. 7).

Considering a regional geothermal gradient of 28–30°/km (Ulmishek (1984) for the Tarim; Christelle Tiberi, personal communication, for Mongolia-Baikal region) the top of this section remained within a few 100 m from the present surface since Middle to Upper

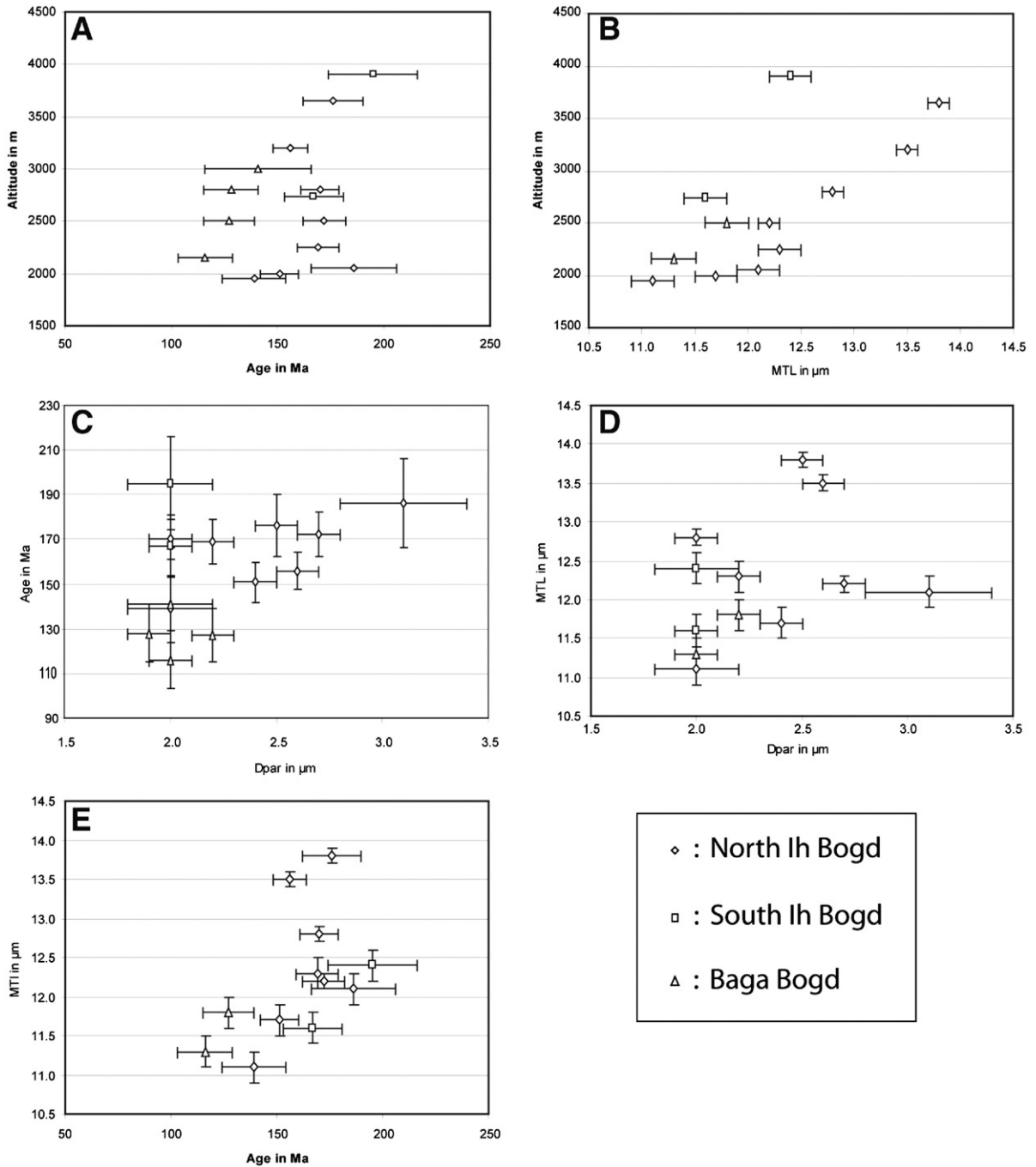


Fig. 5. Different plots of the fission track data showing the relationships between altitude, central ages, mean track lengths and Dpar.

Jurassic times. This implies that the erosional surface that constitutes the present plateau must have formed just after the Jurassic exhumation and has undergone negligible denudation or sedimentation until the last uplift began. Furthermore, even if during this uplift the denudation rate of the plateau has probably increased,

the lowering of this surface should have not exceeded a few meters. This plateau is therefore one of the oldest preserved erosion surfaces at high altitude in the world and the last vertical movement almost entirely corresponds to surface uplift (England and Molnar, 1990).



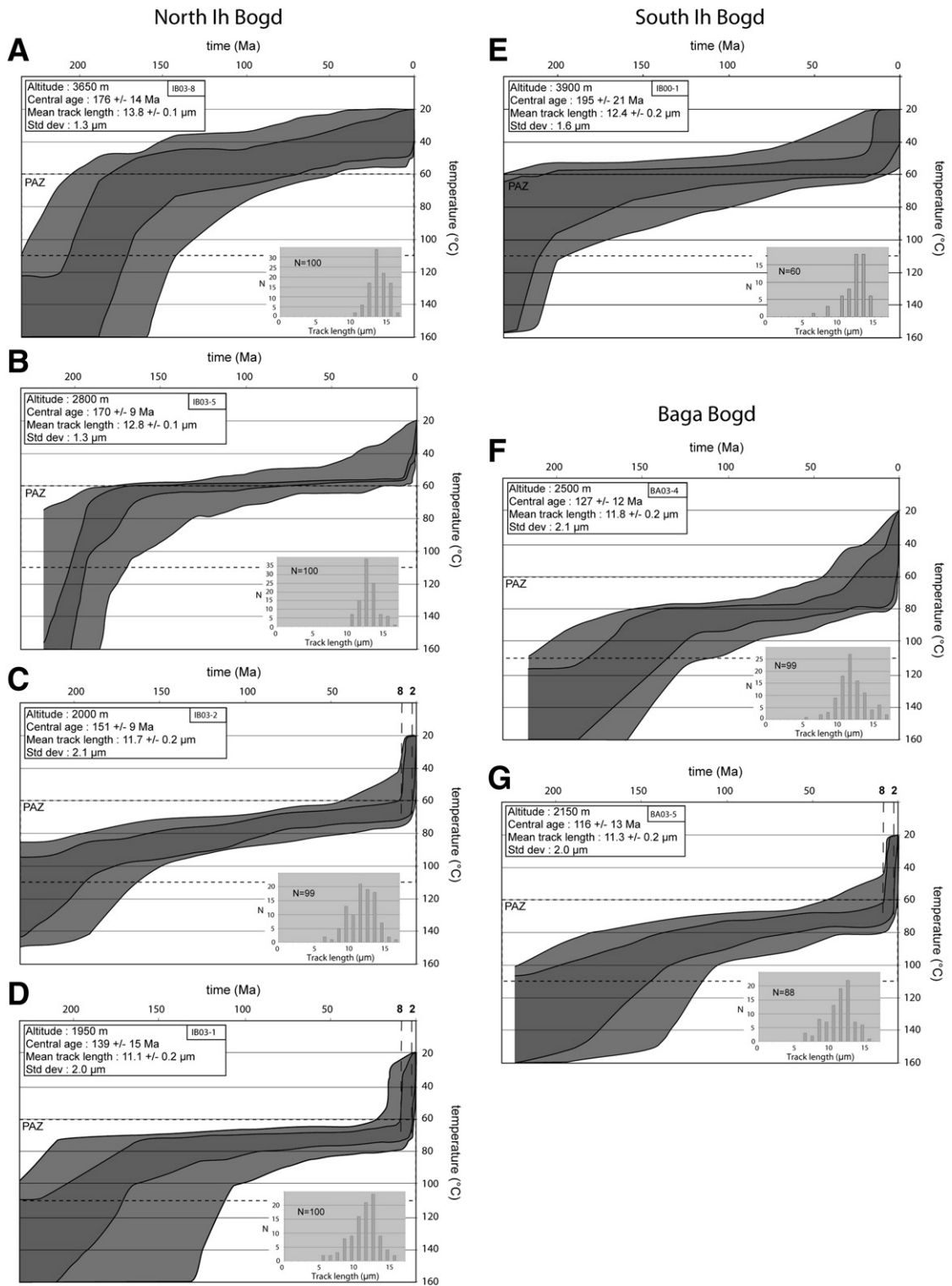


Fig. 6. Cooling paths of some characteristic samples from Ih Bogd and Baga Bogd determined by the modelling of the distribution of the track lengths. The exterior envelop corresponds to  $2\sigma$  uncertainty, the internal envelop corresponds to  $1\sigma$  uncertainty. The validity of the models is limited to the PAZ, i.e. between about  $60^\circ$  and  $110^\circ$   $^\circ\text{C}$ .

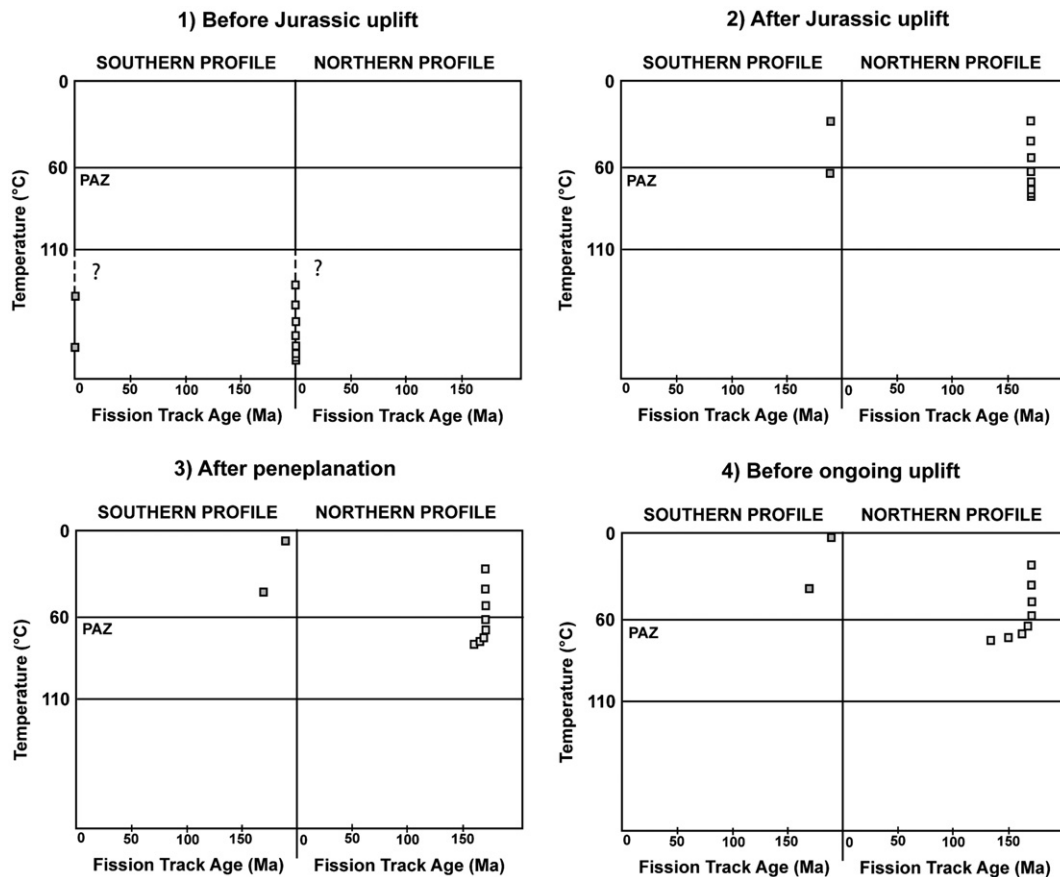


Fig. 7. Evolution of the fission track ages of the samples from South Ih Bogd and North Ih Bogd from the Middle Mesozoic to the Late Cenozoic.

The Lower–Middle Jurassic event that affects the Gobi–Altay has also been observed elsewhere in Central Asia, especially in north Tibet (e.g. (Jolivet et al., 2001; Sobel, 1995; Sobel and Arnaud, 1996; Delville et al., 2001)) and in northwest Altay (e.g. (De Grave and Van den Haute, 2002)). This cooling can be interpreted as a large-scale tectonic event, probably related to the collision that occurred during that period between the Mongolia–Okhotsk region and Siberia (Halim et al., 1998; Zorin, 1999).

The last cooling event, recorded by the samples that were still in the PAZ when it started, refers to the present tectonic deformation and mountain building. The best estimate for the age of onset of this tectonic event is well determined at  $5 \pm 3$  Ma ( $1\sigma$ ), based on the best fitting modelled thermal histories (Fig. 6C, D and G). Important discussions have recently taken place in the literature on whether or not a modelling artefact could generate an overestimated last cooling event (e.g. (Kohn et al., 2002; Gunnell et al., 2003)). This can be especially important when modelling samples with

significantly old central ages ( $>200$  Ma) and mean range MTLs (around  $12 \mu\text{m}$ ) (Gunnell et al., 2003), which is the case for our samples. The main problem discussed for example in Gunnell et al. (2003) is that the initial length of  $16.3 \mu\text{m}$  used in Laslett et al. (1987) annealing model might be too long. The model would thus underestimate the amount of annealing at temperatures lower than  $50\text{--}60$  °C, artificially increasing the initial temperature of the last cooling event. Gunnell et al. (2003) thus empirically decreased the initial lengths to  $14.5 \mu\text{m}$  to match the MTL of Durango standard apatite on which the Laslett et al. model is based. This artificially shifts the modelled thermal histories towards lower temperatures and thus lowers the importance of the last cooling event. However, the authors admit that “The generality of this point nevertheless demands to be tested in a suitably wide range of settings, as rapid recent cooling may in some cases be real (supported by independent geological evidence) rather than merely an algorithm-related artefact”. The initial track length mostly depends on the composition of the apatite crystals

(Barbarand et al., 2003), and monokinetic models such as the Laslett et al. model (Laslett et al., 1987) assume that all the samples have the same annealing kinetics as the standard used, which is seldom the case (Ketcham et al., 1999). Ketcham et al. (2000) model used in this work allows for variable annealing kinetics and thus seems more efficient in describing the cooling path of an “unknown” sample. Since negligible denudation has

affected the summit plateau of Ih Bogd, the vertical amplitude of this uplift can be estimated at about 2 km. This is consistent with an onset cooling temperature close to 60 °C for the lowest samples of the profile. To summarize, the age  $5 \pm 3$  Ma determined for the onset of the last tectonic event in Gobi-Altay seems reasonably reliable. It is derived from a fission track lengths model that allows for variable annealing kinetics and the

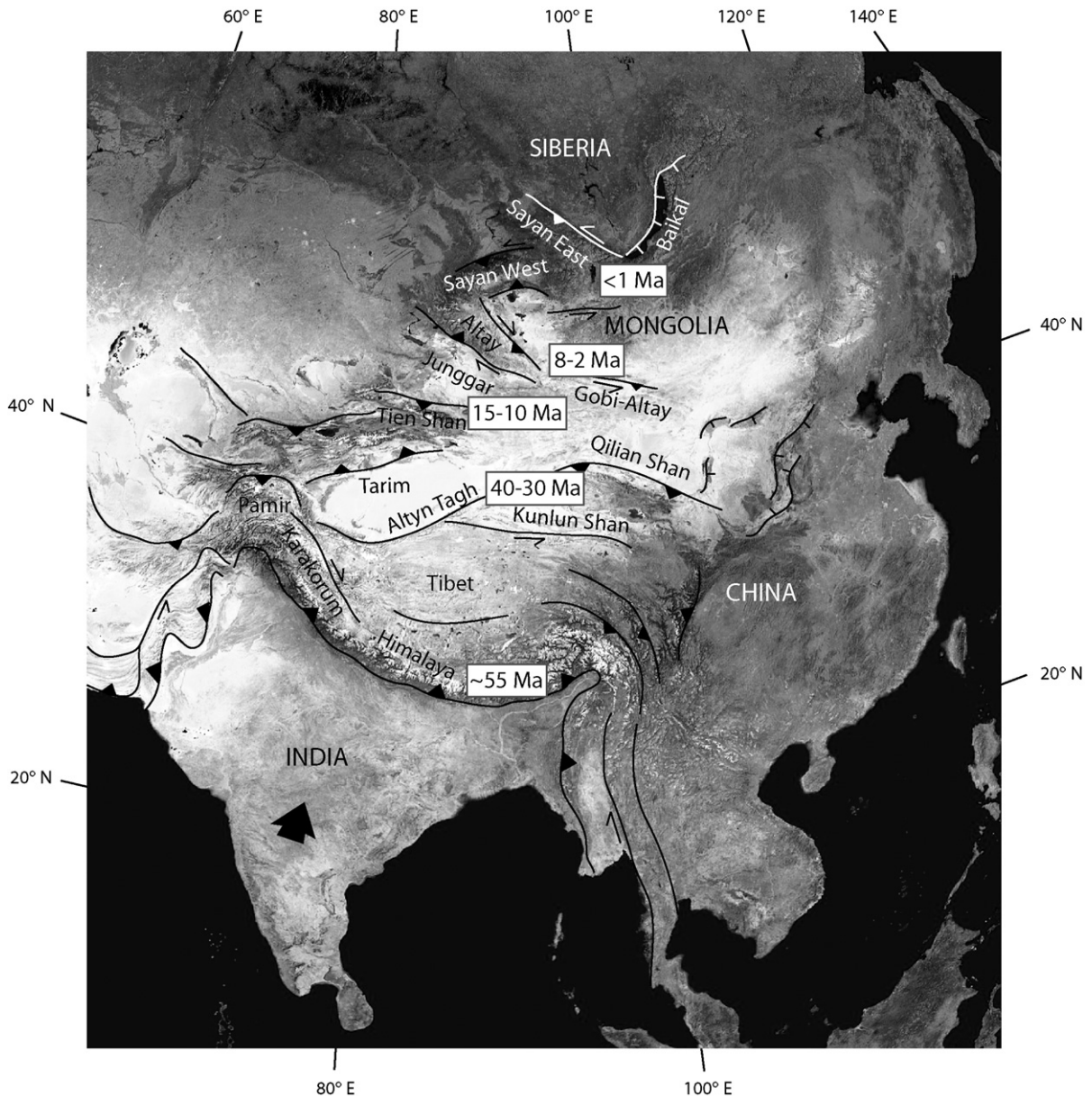


Fig. 8. Simplified tectonic map of Central Asia showing the northward propagation of the Cenozoic transpressive deformation away from the Himalayan collision front towards the Siberian craton ((Patriat and Achache, 1984; Besse et al., 1984; Patzelt et al., 1996; Jolivet et al., 2001; Wang et al., 2004; Avouac et al., 1993; Métivier and Gaudemer, 1997; Sobel and Dumitru, 1997; Bullen et al., 2001; Charreau et al., 2005; Larroque et al., 2001; Arjannikova et al., 2004), this study).

cooling path obtained for the sample fit with independent geological and morphological data.

The Gobi-Altay mountain range appears therefore to be among the youngest relief in Central Asia. This result is consistent with the idea of a sequential northward propagation of the continental deformation triggered by the collision between India and Eurasia 2000 km to the south (e.g. (Tapponnier et al., 2001)) (Fig. 8).

Interestingly, for the last uplift event, samples from Ih Bogd show cooling histories similar to those of Baga Bogd. This means that the massifs of the Gurvan Bogd system – probably including Artz Bogd further east – started to uplift synchronously along the Bogd strike-slip fault. This is consistent with the fact that the Cenozoic deformation along the Bogd fault is controlled by the tectonic reactivation of an ancient structure (e.g. (Cunningham, 1998)).

Fission track data yield a long-term uplift rate of the massifs ranging from 0.25 mm/yr to 1 mm/yr. Even considering the lowest value, this uplift rate is higher than the upper Pleistocene vertical slip rates measured on the faults bordering the massif (0.1 to 0.2 mm/yr). The difference might be explained either by a decrease in deformation rate during the upper Pleistocene, or by distribution of vertical movements on several in-sequence faults within the massif. This last hypothesis is supported by the occurrence of large faults within the Ih Bogd massif, one of which has obviously been active during the ongoing deformation phase (Fig. 4).

## 6. Conclusion

Modelling of fission track data from the Gurvan Bogd massifs suggests that the transpressive deformation resulting from the major India–Asia collision to the south affects the Gobi-Altay range since only  $5 \pm 3$  Ma. This mountain range appears therefore to exhibit some of the youngest relief in Central Asia. The ongoing uplift of the Gurvan Bogd massifs ended a protracted period without major crustal vertical movements, itself following a previous deformation phase in Lower to Middle Jurassic times. The geometric relationships between the geological structures and the present massifs morphology together with the similar cooling histories of Ih Bogd and Baga Bogd strongly suggest that the deformation along the Bogd fault reactivates an inherited zone of weakness, along which at least two important phases of vertical movements ( $\geq 2$  km) have occurred.

The erosional surface that constitutes the remnant flat summits of Ih Bogd and Baga Bogd formed just after the Jurassic exhumation and has undergone negligible

denudation or sedimentation until the last uplift began. Moreover, its preservation on large areas at more than 3500 m of altitude suggests very low erosion processes within these massifs during the ongoing uplift.

The long-term Cenozoic uplift rate of the massifs is estimated to lie between 0.25 and 1 mm/yr, which is slightly higher than the upper Pleistocene vertical slip rates of the bordering faults. This implies that either the uplift rate has diminished in the last stages of the massifs evolution or that these faults do not accommodate the totality of the deformation. This latter hypothesis is supported by the observation of the recent activity of thrust faults within the massifs that would increase the uplift rate inside the massifs compared to the uplift rate determined at their boundaries.

## Acknowledgements

This study has been supported by the INSU “Relief de la Terre” project and by the “Dynamique de la Lithosphere” laboratory. We are thankful to Sébastien Carretier and Alain Chauvet for fruitful discussions. We also thank A. Gleadow and an anonymous reviewer for useful comments and criticism that helped us to improve the original manuscript.

## References

- Arjannikova, N., Larroque, C., Ritz, J.-F., Déverchère, J., Stéphan, J.-F., Arjannikov, S., San'kov, V., 2004. Geometry and kinematics of recent deformation in the Mondy-Tunka area (south-western-most Baikal rift zone, Mongolia-Siberia). *Terra Nova* 16, 265–272. doi:10.1111/j.1365-3121.2004.00565.x.
- Avouac, J.-P., Tapponnier, P., Bai, P., You, M., Wang, G., 1993. Active Thrusting and folding along the northern Tien Shan and late Cenozoic rotation of the Tarim relative to Dzungaria and Kazakhstan. *J. Geophys. Res.* 98, 6755–6804.
- Baljinnyam, I., Bayasgalan, A., Borisov, B.A., Cisternas, A., Dem'yanovich, M.G., Ganbaatar, L., Kochetkov, V.M., Kurushin, R.A., Molnar, P., Philip, H., Vashchilov, Yu.Ya., 1993. Ruptures of major earthquakes and active deformation in Mongolia and its surroundings. *Geol. Soc. Am., Memoir* 181.
- Barbarand, J., Carter, A., Wood, I., Hurford, A.J., 2003. Compositional and structural control of fission track annealing in apatite. *Chem. Geol.* 198, 107–137.
- Bayasgalan, A., Jackson, J., Ritz, J.-F., Carretier, S., 1999. ‘Forebergs’, flowers structures, and the development of large intra-continental strike-slip fault: the Gurvan Bogd fault system in Mongolia. *J. Struct. Geol.* 21, 1285–1302.
- Besse, J., Courtillot, V., Pozzi, J.P., Westphal, M., Zhou, Y.X., 1984. Palaeomagnetic estimates of crustal shortening in the Himalayan thrusts and Zangbo Suture. *Nature* 311, 621–626.
- Bullen, M.E., Burbank, D.W., Garver, J.I., Abdrakhmatov, K.Y., 2001. Late Cenozoic tectonic evolution of the northwestern Tien Shan: new age estimates for the initiation of mountain building. *Bull. Geol. Soc. Am.* 113, 1544–1559.

- Carretier, S., 2000. Cycle sismique et surrection de la chaîne de Gurvan Bogd (Mongolie). Approche de la géomorphologie quantitative, PhD thesis, Université de Montpellier 2, p. 324.
- Charreau, J., Chen, Y., Gilder, S., Dominguez, S., Avouac, J.-P., Sen, S., Sun, D., Li, Y., Wang, W.M., 2005. Magnetostratigraphy and rock magnetism of the Neogene Kuitun He section (northwest China): implications for Late Cenozoic uplift of the Tianshan mountains. *Earth Planet. Sci. Lett.* 230, 177–192.
- Cunningham, D.W., 1998. Lithospheric controls on late Cenozoic construction of the Mongolian Altai. *Tectonics* 17, 891–902.
- Cunningham, D., 2005. Active intracontinental transpressional mountain building in the Mongolian Altai: defining a new class of orogen. *Earth Planet. Sci. Lett.* 240, 436–444.
- Cunningham, W.D., Windley, B.F., Dorjnamjaa, D., Badamgarov, G., Saandar, M., 1996. A structural transect across the Mongolian Western Altai: active transpressional mountain building in Central Asia. *Tectonics* 15, 142–156.
- De Grave, J., Van den Haute, P., 2002. Denudation and cooling of the Lake Teletskoye Region in the Altai Mountains (South Siberia) as revealed by apatite fission-track thermochronology. *Tectonophysics* 349, 145–159.
- Delville, N., Arnaud, N., Montel, J.M., Brunel, M., Sobel, E., 2001. Paleozoic to Cenozoic deformation along the Altyn-Tagh Fault in the Altun Shan range, Eastern Qilian Shan, NE Tibet China. In: Hendrix, M.S., Davis, G.A. (Eds.), *Paleozoic and Mesozoic tectonic evolution of central and eastern Asia: From continental assembly to intracontinental deformation*. *Geol. Soc. Am. Memoir* 194, 269–292.
- Dunkl, I., 2002. TRACKKEY: a Windows program for calculation and graphical presentation of fission track data. *Comput. Geosci.* 28, 3–12.
- England, P., Molnar, P., 1990. Surface uplift, uplift of rocks, and exhumation of rocks. *Geology* 18, 1173–1177.
- Fitzgerald, P.G., Baldwin, S.L., Webb, L.E., O'Sullivan, P.B., 2006. Interpretation of (U-Th)/He single grain ages from slowly cooled crustal terranes: a case study from the Transantarctic Mountains of southern Victoria Land. *Chem. Geol.* 225, 91–120.
- Florensov, N.A., Solonenko, V.P., (Eds.) 1965. *The Gobi-Altay Earthquake*, U.S. Dep. of Commer., Washington, D.C.
- Green, P.F., 1985. A comparison of zeta calibration baselines in zircon, sphene and apatite. *Chem. Geol.* 58, 1–22.
- Green, P.F., Crowhurst, P.V., Duddy, I.R., Japsen, P., Holford, S.P., 2006. Conflicting (U-Th)/He and fission track ages in apatite: enhanced He retention, not anomalous annealing behaviour. *Earth Planet. Sci. Lett.* 250, 407–427.
- Gunnell, Y., Gallagher, K., Carter, A., Widdowson, M., Hurford, A.J., 2003. Denudation history of the continental margin of western peninsular India since the early Mesozoic—reconciling apatite fission-track data with geomorphology. *Earth Planet. Sci. Lett.* 215 (2003) 187–201.
- Halim, N., Kravchinsky, V., Gilder, S., Cogné, J.-P., Alexyutin, M., Sorokin, A., Courtillot, V., Chen, Y., 1998. A palaeomagnetic study from the Mongol-Okhotsk region: rotated Early Cretaceous volcanics and remagnetized Mesozoic sediments. *Earth Planet. Sci. Lett.* 159, 133–145.
- Hanks, T., Ritz, J.-F., Kendrick, K., Finkel, R.C., Garvin, C.D., 1997. Uplift rates in a continental interior: faulting offsets of a ~100 ka abandoned fan along the Bogd fault, southern Mongolia. *Proceedings of the Pensose Conference on the Tectonics of Continental Interiors*.
- Hurford, A.J., 1990. Standardization of fission track dating calibration: recommendation by the fission-track working group of the I.U.G.S., Subcommittee on Geochronology. *Chem. Geol.* 80, 171–178.
- Hurford, A.J., Green, P.F., 1983. The zeta age calibration of fission-track dating. *Geoscience* 1, 285–317.
- Jolivet, M., Brunel, M., Seaward, D., Xu, Z., Yang, J., Roger, F., Tapponnier, P., Malavieille, J., Arnaud, N., Wu, C., 2001. Mesozoic and Cenozoic tectonics of the northern edge of the Tibetan plateau: fission track constraints. *Tectonophysics* 343, 111–134.
- Ketcham, R.A., Donelick, R.A., Carlson, W.D., 1999. Variability of apatite fission-track annealing kinetics: III. Extrapolation to geological time scales. *Am. Mineral.* 84, 1235–1255.
- Ketcham, R.A., Donelick, R.A., Donelick, M.B., 2000. AFTSolve: a program for multi-kinetic modeling of apatite fission-track data. *Geol. Mater. Res.* 2 (1).
- Kohn, B.P., Gleadow, A.J.W., Brown, R.W., Gallagher, K., O'Sullivan, P.B., Foster, D.A., 2002. Shaping the Australian crust over the last 300 million years: insights from fission track thermotectonic imaging and denudation studies of key terranes. *Aust. J. Earth Sci.* 49, 697–717.
- Kurushin, R.A., Bayasgalan, A., Ölziybat, M., Enkhuvshin, B., Molnar, P., Bayarsayhan, C., Hudnut, K.W., Lin, J., 1997. The surface rupture of the 1957 Gobi-Altay, Mongolia, earthquake. *Geol. Soc. Am. Spec. Pap.* 320.
- Larroque, C., Ritz, J.-F., Stéphan, J.-F., San'kov, V., Arjannikova, N., Calais, E., Déverchère, J., Loncke, L., 2001. Interaction compression-extension à la limite Mongolie-Sibérie: analyse préliminaire des déformations récentes et actuelles dans le bassin de Tunka. *C.R. Acad. (Paris)* 332, 177–184.
- Laslett, G.M., Green, P.F., Duddy, I.R., Gleadow, A.W.J., 1987. Thermal annealing of fission tracks in apatite, 2. A quantitative analysis. *Chem. Geol.* 65, 1–13.
- Métivier, F., Gaudemer, Y., 1997. Mass transfer between eastern Tien Shan and adjacent basins (central Asia): constraints on regional tectonics. *Geophys. J. Int.* 128, 1–17.
- O'Sullivan, P.B., Parrish, R.R., 1995. The importance of apatite composition and single-grain ages when interpreting fission track data from plutonic rocks: a case study from the Coast Ranges, British Columbia. *Earth Planet. Sci. Lett.* 132, 213–224.
- Patriat, P., Achache, J., 1984. India-Eurasia collision chronology has implications for crustal shortening and driving mechanisms of plates. *Nature* 311, 615–621.
- Patzelt, A., Huamei, L., Junda, W., Appel, E., 1996. Palaeomagnetism of Cretaceous to Tertiary sediments from southern Tibet: evidence for the extent of the northern margin of India prior to the collision with Eurasia. *Tectonophysics* 259, 259–284.
- Ritz, J.F., Bourlès, D., Brown, E.T., Carretier, S., Chery, J., Enhtuvushin, B., Galsan, P., Finkel, R.C., Hanks, T.C., Kendrick, K.J., Philip, H., Raisbeck, G., Schlupp, A., Schwartz, D.P., Yiu, F., 2003. Late Pleistocene to Holocene slip rates for the Gurvan Bulag thrust fault (Gobi-Altay, Mongolia) estimated with <sup>10</sup>Be dates. *J. Geophys. Res.* 108 (B3), 2162. doi:10.1029/2001JB000553.
- Ritz, J.-F., Vassallo, R., Braucher, R., Brown, E., Carretier, S., Bourlès, D.L., 2006. Using In Situ-Produced <sup>10</sup>Be to Quantify Active Tectonics in the Gurvan Bogd Mountain Range (Gobi-Altay, Mongolia). In: Siame, L., Bourlès, D.L., Brown, E.T. (Eds.), *Geological Society of America Special Paper* 415 "In Situ-Produced Cosmogenic Nuclides and Quantification of Geological Processes", pp. 87–110.
- Shuster, D.L., Flowers, R.M., Farley, K.A., 2006. The influence of natural radiation damage on helium diffusion kinetics in apatite. *Earth Planet. Sci. Lett.* 249, 148–161.
- Sobel, E.R., 1995. Basin analysis and apatite fission-track thermochronology of the Jurassic–Paleogene southwestern Tarim Basin, NW China, PhD thesis, Stanford University, 308 p.

- Sobel, E.R., Arnaud, N., 1996. Age controls on origin and cooling of the Altyn Tagh range, NW China. *Geol. Soc. Am. Abstr. Prog.* 28 (7), A67.
- Sobel, E.R., Dumitru, T.A., 1997. Thrusting and exhumation around the margins of the western Tarim Basin during the India-Asia collision. *J. Geophys. Res.* 102, 5043–5064.
- Tapponnier, P., Molnar, P., 1979. Active faulting and Cenozoic tectonics of the Tien Shan, Mongolian and Baykal regions. *J. Geophys. Res.* 84, 3425–3459.
- Tapponnier, P., Zhiqin, X., Roger, F., Meyer, B., Arnaud, N., Wittlinger, G., Jingsui, Y., 2001. Oblique stepwise rise and growth of the Tibet plateau. *Science* 294, 1671–1677.
- Ulmishek, G., 1984. The geology and petroleum resources of basins in western China: ANL/ES-146, 130 p.
- Vassallo, R., Ritz, J.-F., Braucher, R., Carretier, S., 2005. Dating faulted alluvial fans with cosmogenic  $^{10}\text{Be}$  in the Gurvan Bogd mountain (Gobi-Altay, Mongolia): climatic and tectonic implications. *Terra Nova* 17, 278–285. doi:10.1111/j.1365-3121.2005.00612.x.
- Wang, F., Lo, C.-H., Li, Q., Yeh, M.-W., Wan, J., Zheng, D., Wang, E., 2004. Onset timing of significant unroofing around Qaidam basin, northern Tibet, China: constraints from  $^{40}\text{Ar}/^{39}\text{Ar}$  and FT thermochronology on granitoids. *J. Asian Earth Sci.* 24, 59–69.
- Zorin, Yu.A., 1999. Geodynamics of the western part of the Mongolia-Okhotsk collisional belt, Trans-Baikal region (Russia) and Mongolia. *Tectonophysics* 306, 33–56.